

# Therapeutic effects of eperisone on pulmonary fibrosis via preferential suppression of fibroblast activity

Ken-ichiro Tanaka<sup>1</sup>, Mikako Shimoda<sup>1</sup>, Toshifumi Sugizaki<sup>1</sup>, Maki Ikeda<sup>1</sup>, Ayaka Takafuji<sup>1</sup>, Masahiro Kawahara<sup>1</sup>, NAOKI YAMAKAWA<sup>2</sup>, and Tohru Mizushima<sup>3</sup>

<sup>1</sup>Musashino University

<sup>2</sup>Shujitsu University

<sup>3</sup>LTT Bio-Pharma Co., Ltd

April 05, 2024

## Abstract

**Background and purpose:** Although the exact pathogenesis of idiopathic pulmonary fibrosis (IPF) is still unknown, the transdifferentiation of fibroblasts into myofibroblasts and the production of extracellular matrix components such as collagen, triggered by alveolar epithelial cell injury, are important mechanisms of IPF development. In the lungs of IPF patients, apoptosis is less likely to be induced in fibroblasts than in alveolar epithelial cells, and this process is involved in the pathogenesis of IPF. **Experimental approach:** We used a library containing approved drugs to screen for drugs that preferentially reduce cell viability in LL29 cells (lung fibroblasts from an IPF patient) compared with A549 cells (human alveolar epithelial cell line). **Key results:** After screening, we selected eperisone, a central muscle relaxant used in clinical practice. Eperisone showed little toxicity in A549 cells and preferentially reduced the percentage of viable LL29 cells, while pirfenidone and nintedanib did not have this effect. Eperisone also significantly inhibited transforming growth factor- $\beta$ 1-dependent transdifferentiation of LL29 cells into myofibroblasts. In an in vivo study using ICR mice, eperisone inhibited bleomycin (BLM)-induced pulmonary fibrosis, respiratory dysfunction, and fibroblast activation. In contrast, pirfenidone and nintedanib were less effective than eperisone in inhibiting BLM-induced pulmonary fibrosis under this experimental condition. Finally, we showed that eperisone did not induce adverse effects in the liver and gastrointestinal tract in the BLM-induced pulmonary fibrosis model. **Conclusion and implications:** Considering these results, we propose that eperisone may be safer and more therapeutically beneficial for IPF patients than current therapies.

## Therapeutic effects of eperisone on pulmonary fibrosis via preferential suppression of fibroblast activity

Ken-ichiro Tanaka<sup>1,\*</sup>, Mikako Shimoda<sup>1</sup>, Toshifumi Sugizaki<sup>1</sup>, Maki Ikeda<sup>1</sup>, Ayaka Takafuji<sup>1</sup>, Masahiro Kawahara<sup>1</sup>, Naoki Yamakawa<sup>2</sup>, and Tohru Mizushima<sup>3</sup>.

<sup>1</sup>Laboratory of Bio-Analytical Chemistry, Research Institute of Pharmaceutical Sciences, Faculty of Pharmacy, Musashino University, 1-1-20 Shinmachi, Nishi-Tokyo 202-8585, Japan; <sup>2</sup>Shujitsu University School of Pharmacy, Okayama 703-8516, Japan; <sup>3</sup> LTT Bio-Pharma Co., Ltd, Shiodome Building 3F, 1-2-20 Kaigan, Minato-ku, Tokyo 105-0022, Japan.

## Correspondence

Dr. Ken-ichiro Tanaka, Laboratory of Bio-Analytical Chemistry, Research Institute of Pharmaceutical Sciences, Musashino University, 1-1-20 Shinmachi, Nishitokyo-shi, Tokyo 202-8585, Japan. TEL & FAX: 81-42-468-9335, E-mail:[k-tana@musashino-u.ac.jp](mailto:k-tana@musashino-u.ac.jp)

**Running title** : Eperisone and pulmonary fibrosis

**Keywords:** bleomycin, idiopathic pulmonary fibrosis, fibroblast, eperisone, muscle relaxant.

## Abbreviations

$\alpha$ -SMA,  $\alpha$ -smooth muscle actin; BLM, bleomycin; DAPI, 4,6-diamidino-2-phenylindole; DMBA, 4-dimethylaminobenzaldehyde; DMEM, Dulbecco's modified Eagle's medium; FBS, fetal bovine serum; FoxM1, forkhead box M1; FVC, forced vital capacity; GAPDH, glyceraldehyde-3-phosphate dehydrogenase; HED, human equivalent dose; IPF, idiopathic pulmonary fibrosis; TCA, trichloroacetic acid; Drebrin, developmentally regulated brain protein.

## What is already known

- \* Idiopathic pulmonary fibrosis (Lee, Grabb, Zipfel, & Choi) is a lung disease of unknown etiology with a poor prognosis.
- \* Transdifferentiation of fibroblasts into myofibroblasts and extracellular matrix component production are important IPF development mechanisms.

## What this study adds

- \* Eperisone preferentially suppressed lung fibroblast activity *in vitro*.
- \* Eperisone inhibited bleomycin-induced pulmonary fibrosis without causing adverse effects.

## Clinical significance

- \* Eperisone may be safer and more therapeutically beneficial for IPF patients than current therapies.

## ABSTRACT

**Background and purpose:** Although the exact pathogenesis of idiopathic pulmonary fibrosis (IPF) is still unknown, the transdifferentiation of fibroblasts into myofibroblasts and the production of extracellular matrix components such as collagen, triggered by alveolar epithelial cell injury, are important mechanisms of IPF development. In the lungs of IPF patients, apoptosis is less likely to be induced in fibroblasts than in alveolar epithelial cells, and this process is involved in the pathogenesis of IPF.

**Experimental approach:** We used a library containing approved drugs to screen for drugs that preferentially reduce cell viability in LL29 cells (lung fibroblasts from an IPF patient) compared with A549 cells (human alveolar epithelial cell line).

**Key results:** After screening, we selected eperisone, a central muscle relaxant used in clinical practice. Eperisone showed little toxicity in A549 cells and preferentially reduced the percentage of viable LL29 cells, while pirfenidone and nintedanib did not have this effect. Eperisone also significantly inhibited transforming growth factor- $\beta$ 1-dependent transdifferentiation of LL29 cells into myofibroblasts. In an *in vivo* study using ICR mice, eperisone inhibited bleomycin (BLM)-induced pulmonary fibrosis, respiratory dysfunction, and fibroblast activation. In contrast, pirfenidone and nintedanib were less effective than eperisone in inhibiting BLM-induced pulmonary fibrosis under this experimental condition. Finally, we showed that eperisone did not induce adverse effects in the liver and gastrointestinal tract in the BLM-induced pulmonary fibrosis model.

**Conclusion and implications:** Considering these results, we propose that eperisone may be safer and more therapeutically beneficial for IPF patients than current therapies.

## INTRODUCTION

Idiopathic pulmonary fibrosis (IPF) is a lung disease of unknown etiology with a poor prognosis that is characterized by chronic development of severe fibrosis, resulting in a honeycomb lung (Kim, Collard, & King, 2006; Raghu et al., 2015). Steroids and immunosuppressive drugs have long been used to treat IPF, but in many cases, these drugs do not show therapeutic efficacy against IPF progression (Luppi, Cerri, Beghe, Fabbri, & Richeldi, 2004; Raghu et al., 2015; Walter, Collard, & King, 2006). The primary etiology of IPF is thought to be chronic pulmonary fibrosis triggered by chronic injury to airway and alveolar epithelial cells. Therefore, pirfenidone and nintedanib, antifibrotic agents that have been shown to significantly improve the reduction of forced vital capacity (FVC) in large clinical trials, are being used to treat IPF in clinical practice (Noble et al., 2011; Raghu et al., 2015; Richeldi et al., 2014). However, in some cases, these drugs have not shown efficacy and have been reported to induce adverse effects such as elevation of liver damage markers, diarrhea, and indigestion (Noble et al., 2011; Richeldi et al., 2014). Thus, safer drugs eliciting a therapeutic effect equal to or greater than that of these two approved drugs are necessary.

Although the exact cause of IPF is unknown, it is thought to be triggered by damage to the lung epithelium as a result of increased oxidative stress and the repair and remodeling processes, such as collagen synthesis, that are induced to manage this damage. In other words, this process is overstimulated, resulting in abnormal wound repair and remodeling characterized by collagen deposition, which leads to the development and exacerbation of pulmonary fibrosis (Kinnula & Myllarniemi, 2008; Sheppard, 2006). The cells that play the greatest role in this fibrosis-promoting process are myofibroblasts. Peribronchial and perivascular fibroblasts transdifferentiate (activate) into myofibroblasts in response to various stimuli, especially TGF- $\beta$ 1, and accumulate extracellular matrix components, especially collagen fibers, which are involved in fibrosis (Hinz et al., 2007; Kisseleva & Brenner, 2008). Furthermore, the "apoptosis paradox" is also a possible mechanism of abnormal fibrosis in IPF patients. Apoptosis is preferentially observed in alveolar epithelial cells in the lungs of IPF patients, while little apoptosis occurs in fibroblasts. This produces a relative imbalance resulting in increased fibroblasts in the lungs of IPF patients, which is thought to be involved in the pathogenesis of IPF (Maher et al., 2010; Thannickal & Horowitz, 2006). Thus, it is important to identify compounds that inhibit transdifferentiation of fibroblasts into myofibroblasts or inhibit activation of myofibroblasts. In addition, compounds that are not toxic to alveolar epithelial cells but exert their effects preferentially on lung fibroblasts are promising candidates for IPF therapy.

On the basis of these requirements, we implemented an innovative research strategy (drug repositioning) to identify and develop new IPF therapeutics by screening drugs currently in clinical use to treat other diseases (Mizushima, 2011; Pushpakom et al., 2019). The major advantage of this strategy is that the clinical safety of the drugs screened is already understood, and the risk of unexpected adverse effects in humans can be greatly reduced when these drugs are applied to treat other diseases (Mizushima, 2011; Pushpakom et al., 2019). Using this strategy, we screened drugs not only for IPF but also chronic obstructive pulmonary disease, functional dyspepsia, and irritable bowel syndrome from a library of approved drugs, identified effective drugs for each disease, and analyzed the mechanisms by which these drugs exert their efficacy (Asano et al., 2017; Sugizaki et al., 2019; K. Tanaka et al., 2013; K. I. Tanaka et al., 2017). Recently, other research groups have used this strategy to develop novel therapeutics for coronavirus infection 2019, and candidate drugs have been discovered, including the influenza virus treatment drug remdesivir and the antiparasitic drug ivermectin (Alam et al., 2021). Therefore, we suggest that this strategy is useful for discovering new candidates for treatment of human diseases.

In our previous study, we screened compounds capable of more potently inhibiting the growth of lung fibroblasts (LL29 cells) than that of lung alveolar epithelial cells (A549 cells) and identified idebenone, which has previously been used clinically as a brain metabolic stimulant, from a library of medications already in clinical use. In addition, intratracheal administration of idebenone to mice inhibited bleomycin (BLM)-induced pulmonary fibrosis and decreased FVC (Sugizaki et al., 2019). Furthermore, in our previous screening, we found that, in addition to idebenone, the central muscle relaxant eperisone also acts preferentially on lung fibroblasts. No studies have been conducted on eperisone to determine its effects on fibroblasts or pulmonary fibrosis. Therefore, in this study, we investigated the effect of eperisone, which preferentially induces fibroblast cell death, on BLM-induced pulmonary fibrosis. In addition, we examined its adverse effects by analyzing

plasma markers and the gastrointestinal mucosal status when eperisone was administered to BLM-induced pulmonary fibrosis model mice.

## Materials and Methods

### Chemicals and animals

Eperisone hydrochloride, tolperisone hydrochloride, isoflurane, Dulbecco's modified Eagle's medium (DMEM), L-hydroxyproline, sodium acetate, trichloroacetic acid (TCA), perchloric acid, and formalin neutral buffer solution were obtained from Fujifilm Wako Pure Chemical Corporation (Tokyo, Japan). Tizandine hydrochloride, baclofen, methocarbamol and pirfenidone were from Tokyo Chemical Industry (Tokyo, Japan), and nintedanib was from Cayman Chemical (Ann Arbor, MI). Inaperizone hydrochloride and lanperizone hydrochloride were synthesized in our laboratory. Details of the synthesis method are described in the Supplementary Materials and Methods. BLM was from Nippon Kayaku (Tokyo, Japan). Chloramine T and 4-dimethylaminobenzaldehyde (DMBA) were obtained from Sigma (St. Louis, MO). Fetal bovine serum (FBS) was purchased from BioWest (Nuaille, France), and Ham's F-12K (Kaighn's modification) medium was from Thermo Fischer Scientific (Waltham, MA). An antibody against  $\alpha$ -smooth muscle actin ( $\alpha$ -SMA) was from Abcam (Cambridge, Cambridgeshire), and Alexa Fluor 594 goat anti-rabbit immunoglobulin G were from Invitrogen (Carlsbad, CA). Recombinant human TGF- $\beta$ 1 were from R&D Systems (Minneapolis, MN), and mounting medium for immunohistochemical analysis (VECTASHIELD) was purchased from Vector Laboratories (Burlingame, CA). Mayer's haematoxylin, 1% eosin alcohol solution, primary mordant agent, secondary mordant agent, 0.75% Orange G solution, Masson's staining solution B, 2.5% phosphotungstic acid solution, aniline blue solution, mounting medium for histological examination (malinol) and Weigert's iron haematoxylin were from MUTO Pure Chemicals (Tokyo, Japan). 4,6-diamidino-2-phenylindole (DAPI) was purchased from Dojindo (Kumamoto, Japan). The RNeasy kit was obtained from Qiagen (Valencia, CA), PrimeScript II 1<sup>st</sup> strand cDNA Synthesis kit was from TAKARA Bio (Ohtsu, Japan), and THUNDERBIRD<sup>®</sup> SYBR qPCR Mix was from Bio-Rad (Hercules, CA). ICR mice (6-7 weeks old, male) were purchased from Charles River (Yokohama, Japan). The experiments and procedures described here were carried out in accordance with the Guide for the Care and Use of Laboratory Animals as adopted and promulgated by the National Institutes of Health, and were approved by the Animal Care Committee of Musashino University.

### Cell culture

A549 cells (human lung epithelial cell line) or LL29 cells (lung fibroblasts from an IPF patient) were cultured in DMEM supplemented with 10% FBS or Ham's F-12K (Kaighn's Modification) medium supplemented with 15% FBS, respectively, in a humidified atmosphere of 95% air with 5% CO<sub>2</sub> at 37°C.

Viable cells were measured as previously described (Nakano et al., 2020; K. I. Tanaka et al., 2019). Briefly, dissociated A549 or LL29 cells were added to 96-well culture plates at a concentration of  $1 \times 10^4$  cells per well in 200  $\mu$ l of culture medium. After a 24-h incubation, cells were treated with various reagents added to the medium. After 24 h, the percentage of viable cells was quantified using CellTiter-Glo<sup>®</sup> 2.0 (Promega Corporation, Madison, WI, USA). The cytotoxicity in LL29 cells after eperisone addition was measured every hour using CellTox Green Dye (Promega Corporation, Madison, WI, USA) and a microplate reader (Tecan, Kawasaki, Japan; excitation: 485 nm, emission: 530 nm).

### Real-time RT-PCR analysis

Total RNA was extracted from LL29 cells using an RNeasy kit (Qiagen, Hilden, Germany) according to the manufacturer's protocol. Using a PrimeScript II 1<sup>st</sup> strand cDNA Synthesis kit, samples were reverse-transcribed and THUNDERBIRD(r) SYBR qPCR Mix, Bio-Rad's CFX96 Real-time system, and CFX Manager software (Hercules, CA) were used for real-time RT-PCR experiments. Electrophoretic analysis of reaction products was done to confirm specificity. Glyceraldehyde-3-phosphate dehydrogenase (GAPDH) cDNA was used as an internal standard. Primers were designed using either Primer3 or Primer-BLAST. Primer sequences will be provided upon request.

## Treatment of mice with BLM, eperisone, and other reagents

Mice were anesthetized with isoflurane and intratracheally administered BLM (1 mg/kg, once) in sterile saline via a single channel pipette (P200). Ten days after BLM administration, eperisone (15 or 50 mg/kg), tolperisone (15 mg/kg), pirfenidone (200 mg/kg), and nintedanib (30 mg/kg) were administered orally for a total of 9 days from day 10 to day 18. Various analyses were then performed on day 20.

In the adverse effect study, 10 days after BLM administration, 250 mg/kg of eperisone was orally administered once, which was five times the dose that showed efficacy. Twenty-four hours after eperisone administration, the fecal condition of the mice was visually examined. In addition, plasma samples and stomach and colon tissues were collected from the mice. Analysis of the plasma samples was performed by TRANS GENIC INC. (<https://www.transgenic.co.jp/>).

## Histological and immunohistochemical analyses

Tissue samples were fixed in 10% formalin neutral buffer solution for 24 h, and then embedded in paraffin before being cut into 4  $\mu\text{m}$ -thick sections.

For staining of collagen (Masson's trichrome staining), sections were treated sequentially with primary mordant agent, Weigert's iron haematoxylin, secondary mordant agent, 0.75% Orange G solution, Masson's staining solution B, 2.5% phosphotungstic acid solution, and finally with aniline blue solution. Samples were mounted with malinol, and inspected with a fluorescence microscope (Olympus DP71) or scanned using a NanoZoomer-XR digital slide scanner. Image J software (National Institutes of Health, Bethesda, MD) was used to calculate the percentage of collagen positive area.

For immunohistochemical analysis of  $\alpha$ -SMA, sections were blocked with 2.5% goat serum for 10 min, incubated for 12 h with an antibody against  $\alpha$ -SMA (1:100 dilution) in the presence of 2.5% bovine serum albumin, and then incubated with Alexa Fluor 594 goat anti-rabbit immunoglobulin G (1:500 dilution) and DAPI (5  $\mu\text{g}/\text{ml}$ ) for 1 h. Samples were mounted with VECTASHIELD and inspected with a fluorescence microscope (Olympus DP71). Image J software (National Institutes of Health, Bethesda, MD) was used to calculate the percentage of  $\alpha$ -SMA positive area.

For histological examination, sections were stained first with Mayer's haematoxylin and then with 1% eosin alcohol solution (H&E staining). Samples were mounted with malinol and inspected with a fluorescence microscope (Olympus DP71).

## Measurement of lung mechanics and FVC

Measurement of lung mechanics and FVC was performed with a computer-controlled small-animal ventilator connected to a negative pressure reservoir (FlexiVent; SCIREQ, Montreal, Canada), as previously described (K. Tanaka, Azuma, Miyazaki, Sato, & Mizushima, 2012). Mice were anaesthetised with three types of mixed anesthetic agents (0.75 mg/kg medetomidine, 4.0 mg/kg midazolam, and 5.0 mg/kg butorphanol), a tracheotomy was performed, and an 8 mm-long section of metallic tube (outer and inner diameters of 1.27 mm and 0.84 mm, respectively) was inserted into the trachea. Mice were mechanically ventilated at a rate of 150 breaths/min, using a tidal volume of 8.7 ml/kg and a positive end-expiratory pressure of 2–3  $\text{cmH}_2\text{O}$ .

Total respiratory system elastance and tissue elastance were measured by snap shot and forced oscillation techniques, respectively. For determination of FVC, lungs were inflated to 30  $\text{cmH}_2\text{O}$  over one second and held at this pressure. After 0.2 sec, the pinch valve (connected to the ventilator) was closed, and after 0.3 sec, the shutter valve (connected to the negative pressure reservoir) was opened, exposing the lung to the negative pressure, which was held for 1.5 sec to ensure complete expiration. All data were analysed using FlexiVent software (version 5.3; SCIREQ, Montreal, Canada).

## Hydroxyproline determination

Hydroxyproline content was determined as previously described (Woessner, 1961). Briefly, the lung was removed and homogenised in 1.0 ml of 5% trichloroacetic acid. After centrifugation, pellets were hydrolysed

in 0.5 ml of 10 N HCl for 16 h at 110°C. Each sample was incubated for 20 min at room temperature with 0.5 ml of 1.4% w/v chloramine T solution, and then incubated at 65°C for 10 min with 0.5 ml of Ehrlich's reagent (1 M DMBA, 70% v/v isopropanol and 30% v/v perchloric acid). The absorbance of each sample was then measured at 550 nm to determine the amount of hydroxyproline present.

### Statistical analysis

All values are expressed as mean  $\pm$  S.E.M. One-way ANOVA, followed by Dunnett's test, or Student's unpaired *t*-test were used to evaluate differences between three or more groups or between two groups, respectively. Mac statistical analysis Ver.3.0 software (Esumi Co., Ltd., Tokyo, Japan) was used for the statistical analyses. Differences were considered to be significant when  $P < 0.05$ .

## RESULTS

### Preferential suppression of fibroblast activity by eperisone

A library of drugs already in clinical use was screened to identify drugs that are not toxic to alveolar epithelial cells but are preferentially toxic to lung fibroblasts. Specifically, LL29 or A549 cells were treated with each drug, and 24 h later, the percentages of viable cells were determined using the methylthiazole tetrazolium reagent. Among the drugs that showed lower IC50 values in LL29 cells than in A549 cells, idebenone and eperisone were selected based on the difference in IC50 values between the two cell types, their clinical safety, and other pharmacological activities. As described above, we previously reported the preferential suppression of fibroblast activity by idebenone and its efficacy against BLM-induced pulmonary fibrosis (Sugizaki et al., 2019). Therefore, in this study, we focused on eperisone, which is used in clinical practice as a central muscle relaxant (Iwase, Mano, Saito, & Ishida, 1992), and examined its efficacy against IPF using *in vitro* and *in vivo* systems.

As shown in Figure 1A, eperisone treatment (25–200  $\mu$ M) decreased the percentage of viable LL29 cells in a dose-dependent manner. In contrast, the percentage of viable A549 cells treated with 200  $\mu$ M of eperisone was  $88.5 \pm 3.0\%$  (mean  $\pm$  SEM,  $n = 4$ ), revealing almost no decrease in viable A549 cells after eperisone treatment. We next examined eperisone-induced cytotoxicity in LL29 cells using CellTox Green Dye, which can detect cell membrane disruption. As shown in Figure 1B, LL29 cells treated with eperisone exhibited cytotoxic effects in a time- and concentration-dependent manner. Furthermore, we compared the effect of eperisone on TGF- $\beta$ 1-induced activation of lung fibroblasts. LL29 cells were pre-treated with eperisone (10–30  $\mu$ M), followed by the addition of TGF- $\beta$ 1 (5  $\mu$ M), and the expression of fibrosis-related factors was analyzed 72 h later by real-time RT-PCR. As shown in Figure 1C, TGF- $\beta$ 1 increased the mRNA expression of Collagen 1a1 (*COL1A1*),  $\alpha$ -SMA (*ACTA2*), connective tissue growth factor (*CTGF*), vascular endothelial growth factor (*VEGF*), basic fibroblast growth factor (*BFGF*), and platelet derived growth factor (*PDGF-A*) in LL29 cells, but this increase was suppressed by pre-treatment with eperisone. These results suggest that eperisone preferentially suppressed lung fibroblast activity *in vitro*.

### Effects of other drugs on lung fibroblast viability

As described in the introduction, pirfenidone and nintedanib have been used as anti-fibrotic agents in clinical practice to treat IPF patients. Thus, to investigate the characteristic effect of eperisone on lung fibroblasts, we measured the percentages of viable LL29 and A549 cells after treatment with these existing drugs. After pirfenidone treatment (up to 2 mM), almost no decrease was observed in the percentage of viable cells of both cell types. In contrast, nintedanib decreased the percentage of viable cells of both cell types, but there was no difference in the degree of decrease between the cell types (Figure 2A).

Eperisone is a central muscle relaxant that has been used in clinical practice to improve muscle tone in patients with lumbago and spastic paralysis caused by cerebrovascular disease. Thus, we determined whether other central muscle relaxants exert preferential effects on fibroblasts. Among the six drugs examined, tolperisone, inaperisone, and lanperisone preferentially reduced the viability of LL29 cells, similar to eperisone. However, tizanidine, methocarbamol, and baclofen, at concentrations up to 2 mM, did not reduce the viability of either cell type (Figure 2B). As will be discussed in detail later, because preferential

suppression of fibroblasts was not observed for some central muscle relaxants, we speculate that eperisone exerts its preferential effects by a molecular mechanism other than its muscle relaxant effect.

### **Effect of eperisone on BLM-induced pulmonary fibrosis**

Pulmonary fibrosis was induced by intratracheal administration of BLM to male ICR mice. Specifically, 10 days after BLM administration, mice were divided into three groups based on the rate of change in body weight (excluding the vehicle group), and the effect of oral eperisone administration on lung fibrosis was examined. At 20 days after BLM administration, lung tissue sections were prepared and stained for collagen using Masson's trichrome stain. Collagen deposition in the lungs was observed in a BLM administration-dependent manner. In contrast, oral eperisone administration suppressed the BLM-dependent collagen deposition in a dose-dependent manner (Figure 3A and 3B). Next, we performed quantitative analysis of hydroxyproline, a collagen-specific amino acid, in lung tissue. As shown in Figure 3C, BLM treatment significantly increased the amount of hydroxyproline in lung tissue, while eperisone treatment suppressed this increase. When considering the clinical application of eperisone for the treatment of lung fibrosis, it is important to improve respiratory function as well as histological and biochemical indices. Moreover, our previous analysis showed that lung elastance is increased and FVC is decreased in BLM-induced pulmonary fibrosis (Sugizaki et al., 2019; K. I. Tanaka et al., 2017). Thus, we measured the respiratory function of mice using a computer-controlled ventilator and negative pressure reservoir. As shown in Figure 3D, BLM treatment increased the total elastance (elastance of the entire lung including the bronchi, bronchioles, and alveoli) and tissue elastance (elastance of the alveoli) and decreased the FVC. In contrast, eperisone significantly improved the deterioration of respiratory function induced by BLM administration. These results indicate that eperisone has an ameliorating effect on BLM-dependent pulmonary fibrosis.

Fibroblasts are known to differentiate into myofibroblasts upon activation and play an important role in the development and exacerbation of lung fibrosis (Hinz et al., 2007; Scotton & Chambers, 2007). Thus, we performed an immunohistochemical analysis of  $\alpha$ -SMA, a myofibroblast marker. As shown in Figure 4A, BLM treatment increased the number of  $\alpha$ -SMA-positive cells in the lung, i.e., myofibroblasts increased in a BLM-dependent manner. In contrast, administration of 50 mg/kg eperisone decreased the BLM-dependent increase in  $\alpha$ -SMA-positive cells in the lung to the same level as observed in the vehicle group. These results suggest that eperisone inhibits fibroblast activation not only *in vitro* but also *in vivo* and that it suppresses BLM-dependent pulmonary fibrosis through its inhibitory effect on fibroblast activation.

### **Effects of other drugs on BLM-induced pulmonary fibrosis**

Using the same experimental approach as in Figure 3, we examined the effect of pirfenidone and nintedanib on BLM-dependent pulmonary fibrosis. The dose of pirfenidone (200 mg/kg) was 20 times the initial clinical dose (600 mg/day) used in Japan (Song et al., 2020), and the same dose of nintedanib (30 mg/kg) that had shown triple kinase inhibition in previous animal studies was used (Wollin, Maillet, Quesniaux, Holweg, & Ryffel, 2014). As shown in Supplementary Figure S1A–S1C, BLM-dependent collagen deposition and increased hydroxyproline levels in the lung were not suppressed by oral administration of pirfenidone or nintedanib. Nintedanib or pirfenidone administration tended to improve the BLM-dependent deterioration of respiratory function, but the effect was not statistically significant (Supplementary Figure S1D).

We next analyzed the effect of tolperisone, a structural analogue of eperisone with central muscle relaxant properties (Tekes, 2014), on BLM-dependent pulmonary fibrosis. As shown in Supplementary Figure S2A–S2C, oral administration of tolperisone suppressed BLM-dependent collagen deposition and increased hydroxyproline levels in the lung similar to eperisone administration. In addition, tolperisone significantly improved the BLM-dependent increase in total elastance and tissue elastance and the decrease in FVC (Supplementary Figure S2D). These results indicate that preferential suppression of fibroblast activity is important to prevent BLM-dependent exacerbation of lung fibrosis.

### **Safety analysis of eperisone administration**

In clinical practice, existing IPF treatments, such as pirfenidone and nintedanib, have been reported to

induce adverse effects such as increasing markers of liver damage in the plasma and gastrointestinal disorders (Noble et al., 2011; Richeldi et al., 2014). Therefore, we conducted a comprehensive analysis of markers for pancreatic, hepatic, and renal damage in plasma. The dose of eperisone was five times higher than the dose that showed efficacy for BLM-dependent pulmonary fibrosis. As shown in Table 1, administration of BLM or BLM plus eperisone (250 mg/kg) did not significantly alter 12 plasma markers for pancreatic, hepatic, and renal damage. In addition, no mouse exhibited diarrhea or hemorrhagic stool in either group (Table 2). Furthermore, we also examined gastric and colonic mucosal injury using hematoxylin and eosin staining. As shown in Figure 5 and Table 2, the condition of the gastric and colonic mucosa in mice treated with BLM or BLM plus eperisone (250 mg/kg) was unchanged compared with that in vehicle-treated mice, and no gastric and colonic mucosal injury was observed. These results suggest that eperisone may be able to suppress pulmonary fibrosis without inducing adverse effects.

## DISCUSSION

In this study, we found that eperisone, a central muscle relaxant, preferentially reduces the percentage of viable fibroblasts, an effect not produced by the existing drugs pirfenidone and nintedanib. Moreover, eperisone also inhibited fibroblast activation *in vivo* and markedly reduced BLM-dependent exacerbation of pulmonary fibrosis. Furthermore, no adverse effects were observed, even when eperisone was administered to mice at a dose five times higher than the dose at which it inhibited BLM-induced pulmonary fibrosis. To the best of our knowledge, this is the first study of the effects of eperisone on fibroblasts and its therapeutic effects on a BLM-induced pulmonary fibrosis model. Eperisone is used clinically to improve muscle tone in patients with lumbago and spastic paralysis caused by cerebrovascular disease, and the maximum daily dose used in Japan is 150 mg (orally). Thus, we calculated the human equivalent dose (HED) using the dose used in animals (15 or 50 mg/kg), animal weight (0.04 kg), and human weight (60 kg) according to a previous report (Nair & Jacob, 2016) and found that the HED was 1.3 or 4.5 mg/kg. Therefore, a person weighing 60 kg would require a dosage of 78–270 mg per day. Thus, eperisone at its current clinical dose (150 mg/day) is expected to be effective against IPF.

To investigate whether central muscle relaxation is involved in the preferential effects of eperisone on fibroblasts, we examined the percentage of viable LL29 or A549 cells when other central muscle relaxants were administered. As shown in Figure 3, tolperisone, inaperisone, or lanperisone, but not tizanidine, methocarbamol, or baclofen, preferentially reduced the viability of LL29 cells. Thus, we speculate that eperisone exerts its preferential suppression of fibroblasts by a molecular mechanism other than its muscle relaxant effect. In terms of chemical structure, the drugs that showed fibroblast-preferential effects had higher ClogP values, a lipophilic parameter related to membrane permeability (Supplementary Figure S3). Therefore, a high ClogP value may be necessary for a drug to exert a preferential effect on fibroblasts. In addition, it is interesting to note that the drugs that preferentially reduced the viable percentage of fibroblasts contain isobutyrophenone bound to the nitrogen atom of the heterocyclic ring in the chemical structure. Chemical modification based on this basic structure may lead to the discovery of drugs that preferentially act on fibroblasts.

Nevertheless, the molecular mechanism by which eperisone preferentially reduced the viability of lung fibroblasts could not be elucidated in this study. A recent study suggested that developmentally regulated brain protein (Drebrin), which binds to and increases the stability of actin filaments in neurons, is mainly expressed in myofibroblasts of mouse hearts after myocardial infarction or mouse lungs after BLM administration and promotes the expression of fibrosis-related genes, such as  $\alpha$ -SMA and *Col1A1* (Hironaka et al., 2020). Another group demonstrated that radiation-induced DNA damage is reduced in IPF fibroblasts and correlates with activation of the transcription factor forkhead box M1 (FoxM1) and the subsequent upregulation of the DNA repair proteins RAD51 and BRCA2 (Im, Lawrence, Seelig, & Nho, 2018). Moreover, syndecan-2 is reported to attenuate radiation-induced pulmonary fibrosis in mice and inhibit TGF- $\beta$ 1-induced fibroblast-myofibroblast differentiation, migration, and proliferation by down-regulating phosphoinositide 3-kinase/serine/threonine kinase/Rho-associated coiled-coil kinase signaling and blocking serum response factor binding to the  $\alpha$ -SMA promoter via CD148 (Tsoyi et al., 2017). Furthermore, microRNA-101 has

been reported to inhibit WNT5a (Wnt ligand)-dependent lung fibroblast proliferation by inhibiting NFATc2 signaling and TGF- $\beta$ 1-dependent lung fibroblast activation by inhibiting SMAD2/3 signaling (Huang et al., 2017). Taken together, these reports suggest that the molecular mechanisms by which eperisone preferentially reduces the percentage of viable lung fibroblasts may involve previously reported factors that regulate fibroblast activation.

Although pirfenidone and nintedanib are currently used in clinical practice to treat IPF, in some cases, these drugs have not shown efficacy and have been reported to induce adverse effects such as elevation of liver damage markers, diarrhea, and indigestion (Noble et al., 2011; Richeldi et al., 2014). Thus, in this study, we conducted a "drug-repositioning strategy" to identify safer and more effective drugs for IPF treatment. The *in vitro* studies shown in Figures 1 and 2 revealed that eperisone, but not pirfenidone or nintedanib, exhibited a fibroblast-preferential reduction of viable cells. Moreover, the *in vivo* studies shown in Figure 3 and Supplementary Figure S1 indicated that eperisone, but not pirfenidone or nintedanib, inhibited the exacerbation of BLM-induced pulmonary fibrosis. In addition, eperisone did not induce adverse effects such as hepatotoxicity marker elevation or gastrointestinal disorders. Therefore, we suggest that eperisone may be a safer and more effective treatment for IPF than pirfenidone or nintedanib.

After screening drugs that selectively induce fibroblast cell death, we selected eperisone and showed its efficacy in animal models of IPF, which is caused by fibroblast activation. As mentioned above, eperisone has never been reported to preferentially induce cell death in fibroblasts or effectively treat fibrosis models. However, fibrosis is also induced in organs other than the lungs, such as the liver, heart, and kidneys (Weiskirchen, Weiskirchen, & Tacke, 2019). For example, in the liver, hepatic stellate cells are activated by stimuli such as TGF- $\beta$ 1 and transdifferentiate into myofibroblasts, which promote the production of extracellular matrix components such as collagen and induce liver fibrosis in diseases such as nonalcoholic steatohepatitis (Heyens, Busschots, Koek, Robaey, & Francque, 2021). In the kidney, resident fibroblasts, pericytes, bone marrow-derived cells, and endothelial cells transdifferentiate into myofibroblasts and induce kidney fibrosis (Yuan, Tan, & Liu, 2019). Thus, activated myofibroblasts that transdifferentiate from fibroblasts play a role in promoting fibrosis in organs other than the lungs. Therefore, eperisone, which can preferentially inhibit fibroblast activity, may be effective not only in lung fibrosis models but also in fibrosis models of other organs; thus, the results of this study have promising applications for future research.

## ACKNOWLEDGEMENTS

This research was supported in parts by grants from The Mochida Memorial Foundation for Medical and Pharmaceutical Research, Suzuken Memorial Foundation, and a Grant-in-Aid for Scientific Research from Japan Society for the Promotion of Science (JSPS) (KAKENHI KIBAN (C) 18K06691). We thank Lisa Kreiner, PhD, from Edanz (<https://www.jp.edanz.com/ac>) for editing a draft of this manuscript.

## CONFLICT OF INTEREST

Ken-ichiro Tanaka, Mikako Shimoda, Maki Ikeda, Toshifumi Sugizaki, Ayaka Takafuji, Masahiro Kawahara, and Naoki Yamakawa do not have a financial relationship with a commercial entity that has an interest in the subject of this manuscript. Tohru Mizushima reports receiving personal fees from LTT Bio-Pharma Co., Ltd. during the conduct of the study.

## REFERENCES

- Alam, S., Kamal, T. B., Sarker, M. M. R., Zhou, J. R., Rahman, S. M. A., & Mohamed, I. N. (2021). Therapeutic Effectiveness and Safety of Repurposing Drugs for the Treatment of COVID-19: Position Standing in 2021. *Front Pharmacol*, *12*, 659577. doi:10.3389/fphar.2021.659577
- Asano, T., Tanaka, K. I., Tada, A., Shimamura, H., Tanaka, R., Maruoka, H., ... Takenaga, M. (2017). Ameliorative effect of chlorpromazine hydrochloride on visceral hypersensitivity in rats: possible involvement of 5-HT<sub>2A</sub> receptor. *Br J Pharmacol*, *174* (19), 3370-3381. doi:10.1111/bph.13960
- Heyens, L. J. M., Busschots, D., Koek, G. H., Robaey, G., & Francque, S. (2021). Liver Fibrosis in

Non-alcoholic Fatty Liver Disease: From Liver Biopsy to Non-invasive Biomarkers in Diagnosis and Treatment. *Front Med (Lausanne)*, 8, 615978. doi:10.3389/fmed.2021.615978

Hinz, B., Phan, S. H., Thannickal, V. J., Galli, A., Bochaton-Piallat, M. L., & Gabbiani, G. (2007). The myofibroblast: one function, multiple origins. *Am J Pathol*, 170 (6), 1807-1816. doi: 10.2353/ajpath.2007.070112

Hironaka, T., Ueno, T., Mae, K., Yoshimura, C., Morinaga, T., Horii, Y., ... Nakaya, M. (2020). Drebrin is induced during myofibroblast differentiation and enhances the production of fibrosis-related genes. *Biochem Biophys Res Commun*, 529 (2), 224-230. doi:10.1016/j.bbrc.2020.05.110

Huang, C., Xiao, X., Yang, Y., Mishra, A., Liang, Y., Zeng, X., ... Liu, L. (2017). MicroRNA-101 attenuates pulmonary fibrosis by inhibiting fibroblast proliferation and activation. *J Biol Chem*, 292 (40), 16420-16439. doi:10.1074/jbc.M117.805747

Im, J., Lawrence, J., Seelig, D., & Nho, R. S. (2018). FoxM1-dependent RAD51 and BRCA2 signaling protects idiopathic pulmonary fibrosis fibroblasts from radiation-induced cell death. *Cell Death Dis*, 9 (6), 584. doi:10.1038/s41419-018-0652-4

Iwase, S., Mano, T., Saito, M., & Ishida, G. (1992). Effect of a centrally-acting muscle relaxant, eperisone hydrochloride, on muscle sympathetic nerve activity in humans. *Funct Neurol*, 7 (6), 459-470.

Kim, D. S., Collard, H. R., & King, T. E., Jr. (2006). Classification and natural history of the idiopathic interstitial pneumonias. *Proc Am Thorac Soc*, 3 (4), 285-292. doi: 10.1513/pats.200601-005TK

Kinnula, V. L., & Myllarniemi, M. (2008). Oxidant-antioxidant imbalance as a potential contributor to the progression of human pulmonary fibrosis. *Antioxid Redox Signal*, 10 (4), 727-738. doi: 10.1089/ars.2007.1942

Kisseleva, T., & Brenner, D. A. (2008). Fibrogenesis of parenchymal organs. *Proc Am Thorac Soc*, 5 (3), 338-342. doi: 10.1513/pats.200711-168DR

Luppi, F., Cerri, S., Beghe, B., Fabbri, L. M., & Richeldi, L. (2004). Corticosteroid and immunomodulatory agents in idiopathic pulmonary fibrosis. *Respir Med*, 98 (11), 1035-1044. doi: 10.1016/j.rmed.2004.07.019

Maher, T. M., Evans, I. C., Bottoms, S. E., Mercer, P. F., Thorley, A. J., Nicholson, A. G., ... McNulty, R. J. (2010). Diminished prostaglandin E2 contributes to the apoptosis paradox in idiopathic pulmonary fibrosis. *Am J Respir Crit Care Med*, 182 (1), 73-82. doi:10.1164/rccm.200905-0674OC

Mizushima, T. (2011). Drug discovery and development focusing on existing medicines: drug re-profiling strategy. *J Biochem*, 149 (5), 499-505. doi:mvr032 [pii]

10.1093/jb/mvr032

Nair, A. B., & Jacob, S. (2016). A simple practice guide for dose conversion between animals and human. *J Basic Clin Pharm*, 7 (2), 27-31. doi:10.4103/0976-0105.177703

Nakano, Y., Shimoda, M., Okudomi, S., Kawaraya, S., Kawahara, M., & Tanaka, K. I. (2020). Seleno-l-methionine suppresses copper-enhanced zinc-induced neuronal cell death via induction of glutathione peroxidase. *Metallomics*, 12 (11), 1693-1701. doi:10.1039/d0mt00136h

Noble, P. W., Albera, C., Bradford, W. Z., Costabel, U., Glassberg, M. K., Kardatzke, D., ... Group, C. S. (2011). Pirfenidone in patients with idiopathic pulmonary fibrosis (CAPACITY): two randomised trials. *Lancet*, 377 (9779), 1760-1769. doi:10.1016/S0140-6736(11)60405-4

Pushpakom, S., Iorio, F., Eyers, P. A., Escott, K. J., Hopper, S., Wells, A., ... Pirmohamed, M. (2019). Drug repurposing: progress, challenges and recommendations. *Nat Rev Drug Discov*, 18 (1), 41-58. doi:10.1038/nrd.2018.168

Raghu, G., Rochweg, B., Zhang, Y., Garcia, C. A., Azuma, A., Behr, J., ... Latin American Thoracic, A. (2015). An Official ATS/ERS/JRS/ALAT Clinical Practice Guideline: Treatment of Idiopathic Pulmonary

Fibrosis. An Update of the 2011 Clinical Practice Guideline. *Am J Respir Crit Care Med*, 192 (2), e3-19. doi:10.1164/rccm.201506-1063ST

Richeldi, L., du Bois, R. M., Raghu, G., Azuma, A., Brown, K. K., Costabel, U., ... Investigators, I. T. (2014). Efficacy and safety of nintedanib in idiopathic pulmonary fibrosis. *N Engl J Med*, 370 (22), 2071-2082. doi:10.1056/NEJMoa1402584

Scotton, C. J., & Chambers, R. C. (2007). Molecular targets in pulmonary fibrosis: the myofibroblast in focus. *Chest*, 132 (4), 1311-1321. doi:10.1378/chest.06-2568

Sheppard, D. (2006). Transforming growth factor beta: a central modulator of pulmonary and airway inflammation and fibrosis. *Proc Am Thorac Soc*, 3 (5), 413-417. doi: 10.1513/pats.200601-008AW.

Song, M. J., Moon, S. W., Choi, J. S., Lee, S. H., Lee, S. H., Chung, K. S., ... Kim, S. Y. (2020). Efficacy of low dose pirfenidone in idiopathic pulmonary fibrosis: real world experience from a tertiary university hospital. *Sci Rep*, 10 (1), 21218. doi:10.1038/s41598-020-77837-x

Sugizaki, T., Tanaka, K. I., Asano, T., Kobayashi, D., Hino, Y., Takafuji, A., ... Mizushima, T. (2019). Idefenone has preventative and therapeutic effects on pulmonary fibrosis via preferential suppression of fibroblast activity. *Cell Death Discov*, 5 , 146. doi:10.1038/s41420-019-0226-y

Tanaka, K., Azuma, A., Miyazaki, Y., Sato, K., & Mizushima, T. (2012). Effects of lecithinized superoxide dismutase and/or pirfenidone against bleomycin-induced pulmonary fibrosis. *Chest*, 142 (4), 1011-1019. doi: 10.1378/chest.11-2879

Tanaka, K., Ishihara, T., Sugizaki, T., Kobayashi, D., Yamashita, Y., Tahara, K., ... Mizushima, T. (2013). Mepenzolate bromide displays beneficial effects in a mouse model of chronic obstructive pulmonary disease. *Nat Commun*, 4 , 2686. doi:10.1038/ncomms3686

Tanaka, K. I., Niino, T., Ishihara, T., Takafuji, A., Takayama, T., Kanda, Y., ... Mizushima, T. (2017). Protective and therapeutic effect of felodipine against bleomycin-induced pulmonary fibrosis in mice. *Sci Rep*, 7 (1), 3439. doi:10.1038/s41598-017-03676-y

Tanaka, K. I., Shimoda, M., Kasai, M., Ikeda, M., Ishima, Y., & Kawahara, M. (2019). Involvement of SAPK/JNK Signaling Pathway in Copper Enhanced Zinc-Induced Neuronal Cell Death. *Toxicol Sci*, 169 (1), 293-302. doi:10.1093/toxsci/kfz043

Tekes, K. (2014). Basic aspects of the pharmacodynamics of tolperisone, a widely applicable centrally acting muscle relaxant. *Open Med Chem J*, 8 , 17-22. doi:10.2174/1874104501408010017

Thannickal, V. J., & Horowitz, J. C. (2006). Evolving concepts of apoptosis in idiopathic pulmonary fibrosis. *Proc Am Thorac Soc*, 3 (4), 350-356. doi:10.1513/pats.200601-001TK

Tsoyi, K., Chu, S. G., Patino-Jaramillo, N. G., Wilder, J., Villalba, J., Doyle-Eisele, M., ... Rosas, I. O. (2017). Syndecan-2 Attenuates Radiation-induced Pulmonary Fibrosis and Inhibits Fibroblast Activation by Regulating PI3K/Akt/ROCK Pathway via CD148. *Am J Respir Cell Mol Biol* doi:10.1165/rcmb.2017-0088OC

Walter, N., Collard, H. R., & King, T. E., Jr. (2006). Current perspectives on the treatment of idiopathic pulmonary fibrosis. *Proc Am Thorac Soc*, 3 (4), 330-338. doi: 10.1513/pats.200602-016TK

Weiskirchen, R., Weiskirchen, S., & Tacke, F. (2019). Organ and tissue fibrosis: Molecular signals, cellular mechanisms and translational implications. *Mol Aspects Med*, 65 , 2-15. doi:10.1016/j.mam.2018.06.003

Woessner, J. F., Jr. (1961). The determination of hydroxyproline in tissue and protein samples containing small proportions of this imino acid. *Arch Biochem Biophys*, 93 , 440-447. doi: 10.1016/0003-9861(61)90291-0

Wollin, L., Maillet, I., Quesniaux, V., Holweg, A., & Ryffel, B. (2014). Antifibrotic and anti-inflammatory activity of the tyrosine kinase inhibitor nintedanib in experimental models of lung fibrosis. *Journal of Pharmacology and Experimental Therapeutics*, 349 (2), 209-220. doi:10.1124/jpet.113.208223

Yuan, Q., Tan, R. J., & Liu, Y. (2019). Myofibroblast in Kidney Fibrosis: Origin, Activation, and Regulation. *Adv Exp Med Biol*, 1165 , 253-283. doi:10.1007/978-981-13-8871-2\_12

## Figure legends

### Table 1. Effect of eperisone administration on biochemical markers in the blood.

Mice were treated with bleomycin (BLM, 1 mg/kg) or vehicle once only on day 0. The mice were then orally administered 250 mg/kg of eperisone (Epe) once at day 10. After 24 h, whole blood was collected from the mice. Analysis of the blood samples was performed by TRANS GENIC INC. Values represent the mean  $\pm$  SEM  $**P < 0.01$  ;  $*P < 0.05$  .

### Table 2. Effects of eperisone administration on gastric and colonic mucosa

Mice were treated with bleomycin (BLM, 1 mg/kg) or vehicle once only on day 0. The mice were then orally administered 250 mg/kg of eperisone (Epe) once at day 10. After 24 h, the fecal condition (diarrhea or hemorrhagic stool) of the mice was visually examined. Gastric mucosal injury and colonic mucosal injury were analyzed based on the hematoxylin and eosin staining images shown in Figure 5.

### Figure 1. Preferential suppression of fibroblast activity by eperisone.

LL29 or A549 cells were incubated with the indicated concentrations ( $\mu$ M) of eperisone for 24 h. The percentage of viable cells was determined using a CellTiter-Glo<sup>®</sup> 2.0 assay (A). LL29 cells were incubated with the indicated concentrations ( $\mu$ M) of eperisone for 18 h. The cytotoxicity was measured every hour using CellTox Green Dye and a microplate reader (excitation: 485 nm, emission: 530 nm) (B). LL29 cells were incubated with transforming growth factor (TGF)- $\beta$ 1 (5 ng/ml) for 72 h in the presence of the indicated concentrations of eperisone. Total RNA was extracted and subjected to real-time RT-PCR using a specific primer set for each gene. The values were normalized to *Gapdh* gene expression and expressed relative to the control sample (C). Values represent the mean  $\pm$  SEM  $** P < 0.01$  ;  $*P < 0.05$  ; NS, not significant.

### Figure 2. Effect of other drugs on the percentage of viable LL29 and A549 cells.

LL29 or A549 cells were incubated with the indicated concentrations of pirfenidone, nintedanib (A), tolperisone, inaperisone, lanperisone, tizanidine, methocarbamol, or baclofen (B) for 24 h. The percentage of viable cells was determined using a CellTiter-Glo<sup>®</sup> 2.0 assay. Values represent the mean  $\pm$  SEM  $**P < 0.01$  ;  $*P < 0.05$  .

### Figure 3. Effect of eperisone on pre-developed pulmonary fibrosis.

Mice were treated with bleomycin (BLM, 1 mg/kg) or vehicle once only on day 0. The mice were then orally administered the indicated dose of eperisone (Epe) once daily for 9 days (from day 10 to day 18). Pulmonary tissue sections were prepared on day 20 and subjected to a histopathological examination (Masson's trichrome staining; scale bar = 500  $\mu$ m) (A). The collagen-positive area was determined based on Masson's trichrome staining images (B). The pulmonary hydroxyproline level was determined on day 20 (C). The total respiratory system elastance, tissue elastance, and forced vital capacity (FVC) were measured on day 20 (D). Values represent the mean  $\pm$  SEM  $**P < 0.01$  ;  $*P < 0.05$  ; NS, not significant.

### Figure 4. Effect of eperisone on bleomycin-induced increases in myofibroblasts.

Mice were treated with bleomycin (BLM, 1 mg/kg) or vehicle once only on day 0. The mice were then orally administered the indicated dose of eperisone (Epe) once daily for 9 days (from day 10 to day 18). Pulmonary tissue sections were prepared on day 20 and subjected to immunohistochemical analysis with an antibody against  $\alpha$ -smooth muscle actin (SMA) (scale bar = 100  $\mu$ m) (A). The  $\alpha$ -SMA-positive area was determined using ImageJ software (B). Values represent the mean  $\pm$  SEM  $**P < 0.01$  ;  $*P < 0.05$  .

**Figure 5. Effects of eperisone administration on gastric and colonic mucosa.**

Mice were treated with bleomycin (BLM, 1 mg/kg) or vehicle once only on day 0. The mice were then orally administered 250 mg/kg of eperisone (Epe) once at day 10. After 24 h, the stomach and colon were collected from the mice. Gastric (A) and colonic (B) tissue sections were prepared and subjected to histopathological examination (hematoxylin and eosin staining; scale bar = 200  $\mu$ m).

**Figure 1**

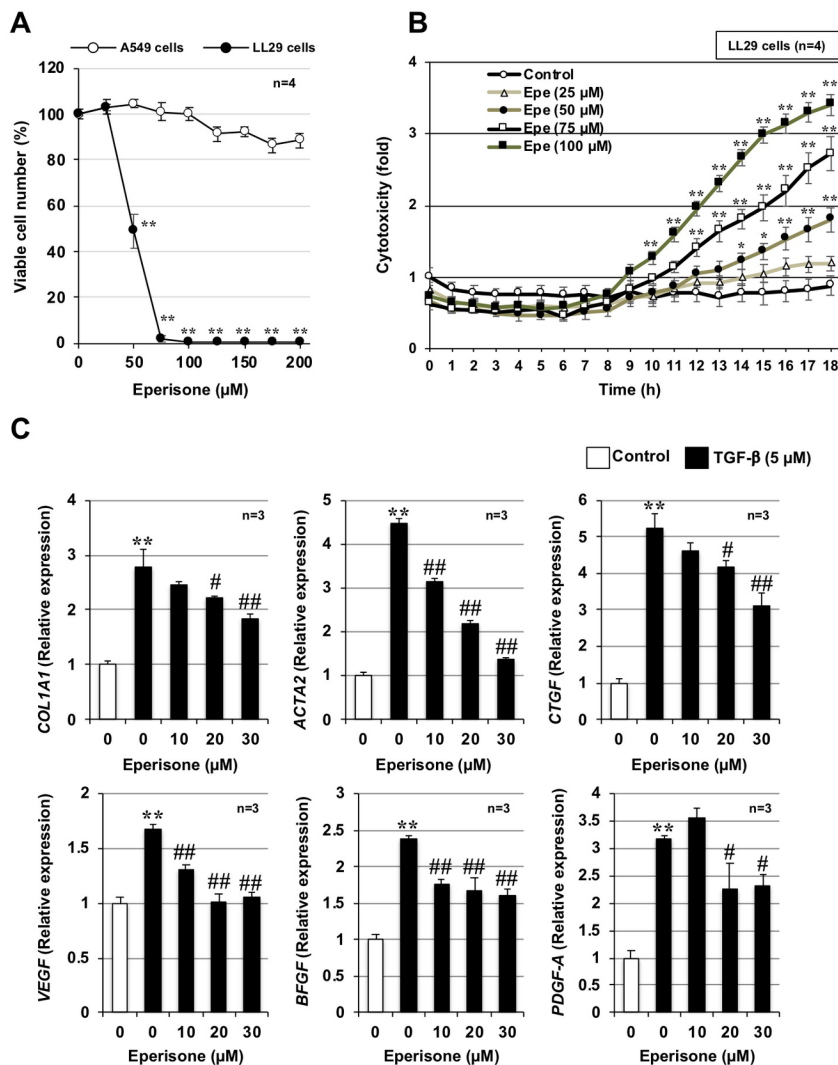


# Figure 2

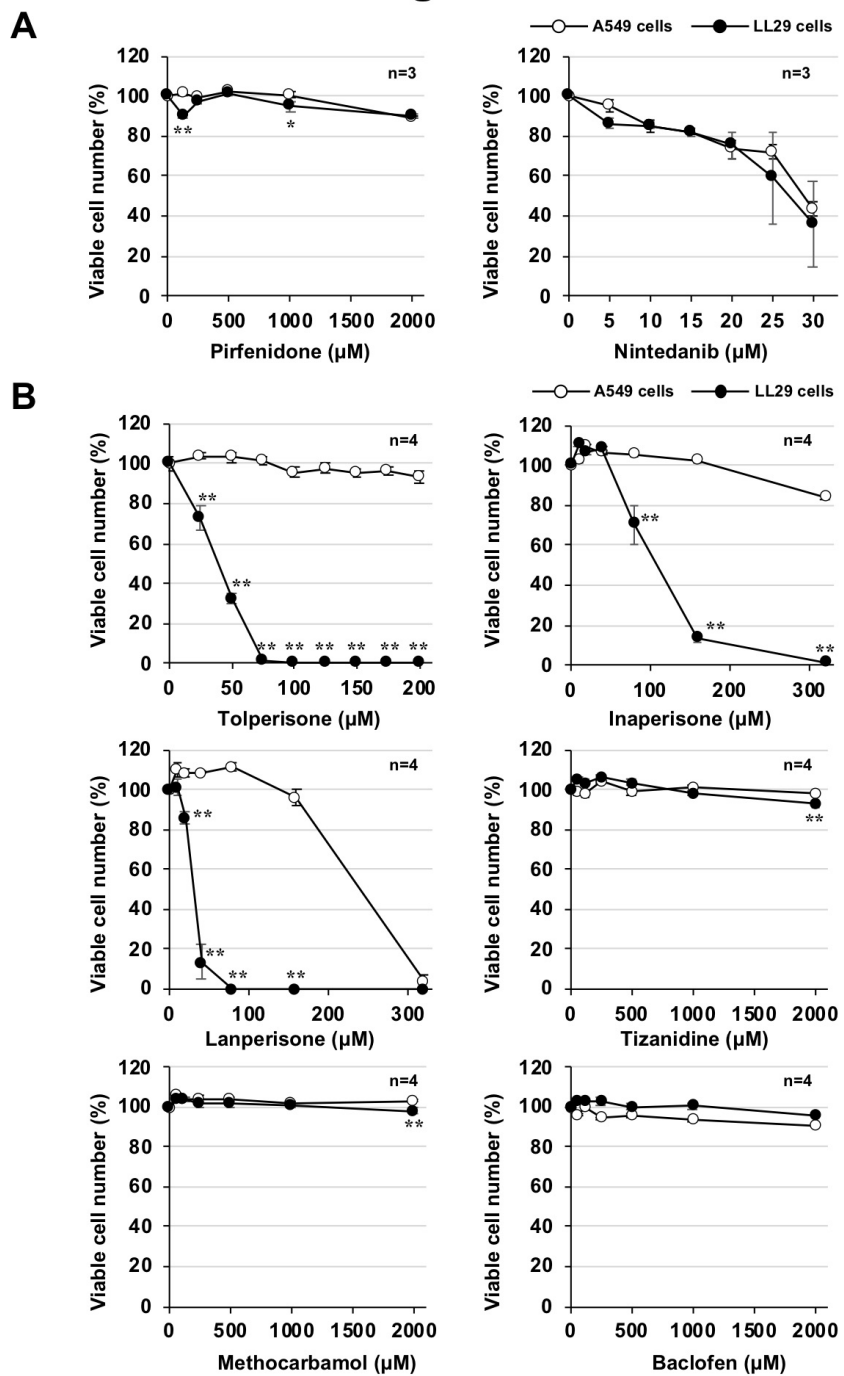
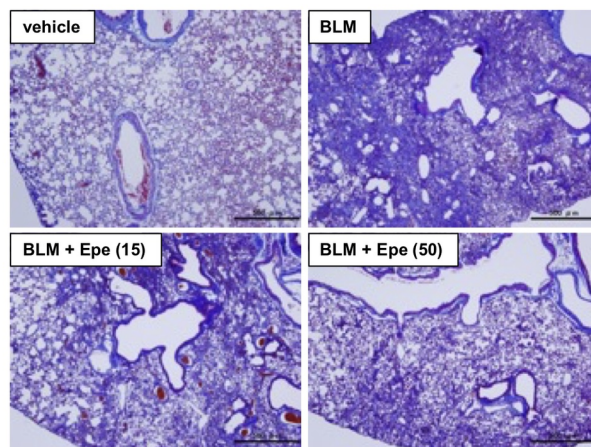
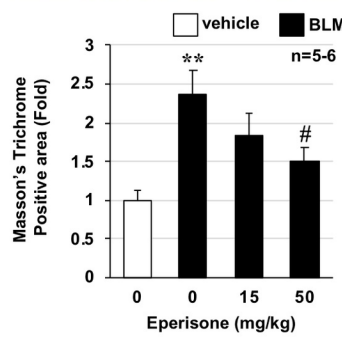


### Figure 3

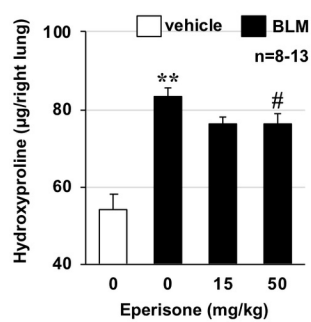
**A**



**B**



**C**



**D**

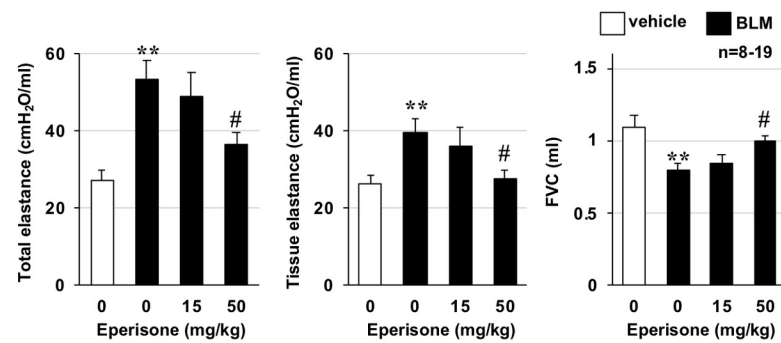


### Figure 4

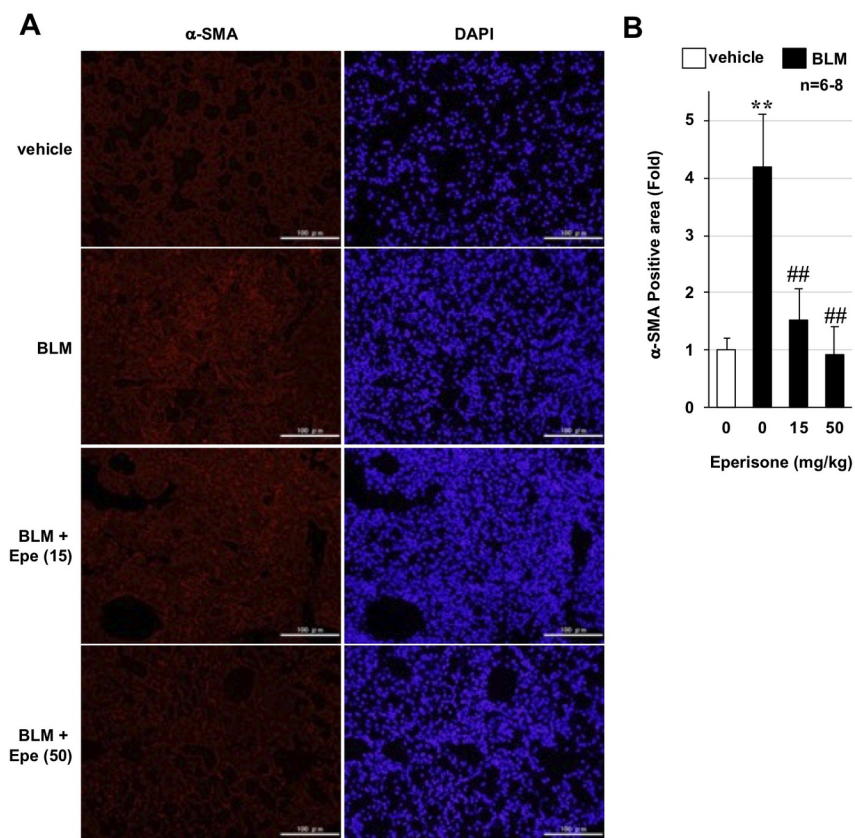


### Figure 5

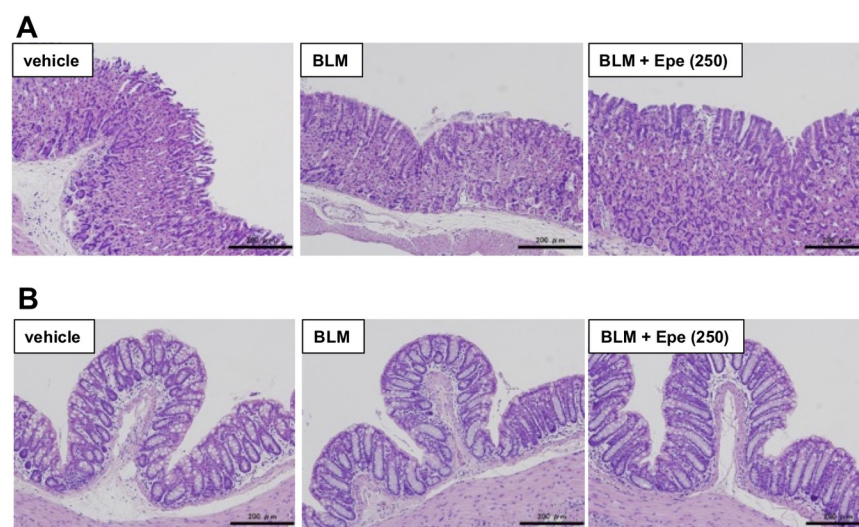


### Table 1

	vehicle (n = 4)	BLM (n = 4)	BLM + Epe (250) (n = 4)
<b>Total protein (g/dL)</b>	5.28 ± 0.40	4.70 ± 0.45	5.65 ± 0.17
<b>Albumin (g/dL)</b>	2.48 ± 0.10	2.28 ± 0.14	2.55 ± 0.03
<b>A/G ratio</b>	0.90 ± 0.04	0.98 ± 0.09	0.83 ± 0.03
<b>Total bilirubin (mg/dL)</b>	> 0.1	> 0.1	> 0.1
<b>AST (U/L)</b>	51.5 ± 7.1	50.5 ± 6.4	55.8 ± 5.0
<b>ALT (U/L)</b>	20.0 ± 1.6	22.8 ± 4.8	22.8 ± 2.5
<b>ALP (U/L)</b>	126.8 ± 14.1	124.3 ± 14.4	98.5 ± 15.6
<b>Amylase (U/L)</b>	2469.5 ± 14.1	2166.8 ± 160.6	2549.3 ± 44.4
<b>BUN (mg/dL)</b>	16.3 ± 0.27	11.3 ± 0.94	13.9 ± 1.13
<b>Creatinine (mg/dL)</b>	> 0.1	> 0.1	> 0.1
<b>Total cholesterol (mg/dL)</b>	119.3 ± 10.5	94.8 ± 7.9	113.3 ± 7.8
<b>Blood glucose (mg/dL)</b>	265.3 ± 50.3	227.3 ± 30.9	317.0 ± 32.4

### Table 2

	vehicle (n = 4)	BLM (n = 4)	BLM + Epe (250) (n = 4)
<b>Diarrhea</b>	n.d.	n.d.	n.d.
<b>Hemorrhagic stool</b>	n.d.	n.d.	n.d.
<b>Gastric mucosal injury</b>	n.d.	n.d.	n.d.
<b>Colonic mucosal injury</b>	n.d.	n.d.	n.d.